



HAL
open science

Pivotal role of H₂ in the isomerisation of isosorbide over a Ru/C catalyst

H. Hu, A. Ramzan, R. Wischert, F. Jérôme, Carine Michel, K. de Olivera Vigier, M. Pera-Titus

► To cite this version:

H. Hu, A. Ramzan, R. Wischert, F. Jérôme, Carine Michel, et al.. Pivotal role of H₂ in the isomerisation of isosorbide over a Ru/C catalyst. *Catalysis Science & Technology*, 2021, 11 (24), pp.7973-7981. 10.1039/D1CY01709H . hal-03428751

HAL Id: hal-03428751

<https://hal.science/hal-03428751>

Submitted on 22 Aug 2022

HAL is a multi-disciplinary open access archive for the deposit and dissemination of scientific research documents, whether they are published or not. The documents may come from teaching and research institutions in France or abroad, or from public or private research centers.

L'archive ouverte pluridisciplinaire **HAL**, est destinée au dépôt et à la diffusion de documents scientifiques de niveau recherche, publiés ou non, émanant des établissements d'enseignement et de recherche français ou étrangers, des laboratoires publics ou privés.

ARTICLE

Pivotal role of H₂ in the isomerisation of isosorbide over Ru/C catalyst

Received 00th January 20xx,
Accepted 00th January 20xx

H. Hu,^{a,b1} A. Ramzan,^{c1} R. Wischert,^a F. Jérôme,^b C. Michel,^{c*} K. de Olivera Vigier,^{b*} M. Pera-Titus^{a*}

DOI: 10.1039/x0xx00000x

Isosorbide isomerisation is a known reaction that can proceed over Ru and Ni-based heterogeneous catalysts. As a rule, an exogenous H₂ pressure (40–100 bar) is required, even though H₂ does not participate stoichiometrically to the reaction. By marrying experiments with DFT computations, we ascribe the role of H₂ in isosorbide isomerisation to a coverage effect at the catalyst surface. We demonstrate the possibility of conducting the reaction at low H₂ pressure either in the presence of an inert gas to increase H₂ solubility in the underlying solvent, or using 2-propanol as hydrogen donor. This might benefit the economy and safety of a potential industrial process.

Introduction

Isosorbide (IS) along with its isomers isomannide (IM) and isoidide (II), collectively referred to as *isohexides*, makes a group of biobased *platform chemicals* that have gained considerable interest over the past two decades as potential replacement to fossil-fuel based products.¹ In particular, isosorbide and its monoamine and diamine derivatives have attracted great interest in the manufacture of biobased polymers such as polyurethanes, polymethacrylates and polyamides, with a possible better environmental footprint compared to fossil-based counterparts.^{1b,2} Isohexides are obtained from acid-catalysed hydration of hexitols D-Sorbitol (IS), D-Mannitol (IM) and L-iditol (II) which in turn can be produced through hydrogenation of monosaccharides, *i.e.* glucose and fructose.¹ Structurally, isohexides consist in two tetrahydrofuran rings *cis*-connected resulting in a rigid V-shaped structure (Scheme 1).^{1,3} The three isomers differ in the relative configuration of the two secondary OH groups: IS has OH groups in opposite (*endo-exo*) orientation relative to the ring skeleton, while IM (*endo-endo*) and II (*exo-exo*) have OH groups pointing in the same direction relative the ring skeleton. Unlike *exo*-OH groups, *endo*-OH groups are better positioned to engage in intermolecular hydrogen bonding with the oxygen atoms of the adjoining furan ring.^{3,4} These structural differences lead to differences in the physicochemical properties and reactivity of isohexides.^{4,5}

The catalytic isomerisation of IS was first described by Fletcher and Goepp in 1946 using Raney nickel for its dehydrogenating properties.^{3c} Wright and Brandner performed the isomerisation in 1964 over Ni-Kieselguhr catalysts and pointed out an equilibrium distribution between the three isomers at *ca.* 55% II, 39% IS and 6% IM.⁶ Such thermodynamics-driven equilibrium distribution is at display in the synthesis of functional bio-based chemicals derived from isohexides.⁷ In this view, understanding the isomerisation mechanism of the three isomers is essential. In addition, the isomerisation presents a viable route to obtain isoidide which has less abundant sugar precursor.^{6a}

The isomerisation of isohexides is believed to proceed via a dehydrogenation-rehydrogenation pathway (H₂-borrowing) (Scheme 1).^{1,3-8} When using a heterogeneous catalyst, since the intermediate (mono, di)ketones are not observed, dehydrogenation is often regarded as the rate-determining step.⁸ An alternative route is the dehydration-rehydration pathway, but it was dismissed by van Es and co-workers since the expected by-products such as unsaturated isohexides or isohexides with OH group in 1-, 3-, 4- or 6-positions were absent in the reaction mixture obtained during the isomerisation of IS using Ru/C in water.⁸ Recently, Rose and co-workers studied in detail the mechanism for IM isomerisation.⁹ Supported by D-exchange experiments, they validated the dehydrogenation-hydrogenation mechanism at 120 °C. Above that temperature, and at a basic pH, full H-D exchange of all protons in IM was observed which they ascribed to a keto-enol equilibrium, thereby hinting at a potential dehydration-rehydration mechanism. Considering that dimethyl isosorbide is also isomerised at similar conditions, the authors proposed an alternative *direct hydride exchange* pathway. The authors hypothesized that α-C–H bond scission results in the formation of a carbenium ion and a surface hydride. The carbenium ion rotates around the C–O bond to facilitate the inversion of the chiral centre before being hydrogenated back. When it comes

^a Eco-Efficient Products and Processes Laboratory (E2P2L), UMI 3464 CNRS-Solvay, 3966 Jin Du Road, Xin Zhuang Ind. Zone, 201108 Shanghai, China. Email: marc.pera-titus-ext@solvay.com

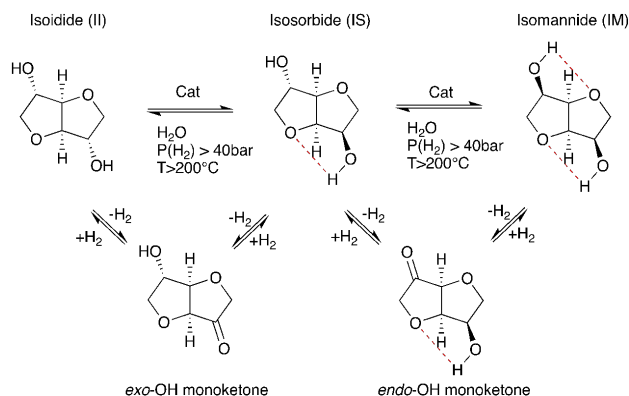
^b IC2MP UMR CNRS_ Université de Poitiers 7285, ENSIP 1 rue Marcel Doré, TSA 41195, 86073 Poitiers Cedex 9, France. Email: karine.vigier@univ-poitiers.fr

^c Univ Lyon, Ecole Normale Supérieure de Lyon, CNRS UMR 5182, Laboratoire de Chimie, F69364 Lyon, France. Email: carine.michel@ens-lyon.fr

¹ These authors contributed equally to the work.

Electronic Supplementary Information (ESI) available: [details of any supplementary information available should be included here]. See DOI: 10.1039/x0xx00000x

to isohexides, this mechanism is difficult to differentiate from dehydrogenation-rehydrogenation and would require a deeper investigation using modelling.



Scheme 1. Structure of isohexide isomers: isomannide (IM) or 1,4:3,6-dianhydro-D-mannitol, isosorbide (IS) or 1,4:3,6-dianhydro-D-sorbitol, and isoidide (II) or 1,4:3,6-dianhydro-L-iditol. A possible isomerisation mechanism is driven by dehydrogenation/rehydrogenation through the mono-ketone intermediates (MK).

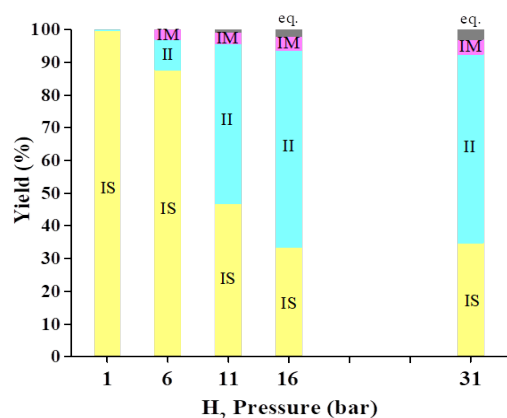


Fig 1. Product distribution and mass loss under different H₂ pressures. Reaction conditions: 1 g IS, 15 mL H₂O, pH 10, 0.05 g Ru/C (5wt %), 200 °C, 1 h.

Very high H₂ pressures (40–100 bar) were necessary to reach equilibrium when using Ni-Kieselguhr to isomerise IS, even if H₂ does participate stoichiometrically to the reaction.⁶ The II yield increased linearly with the pH (8–11) of the initial solution. At pH > 11, poor selectivity was observed due to side reactions, which were not described. Wright and Hartmann reported a similar type of behaviour using the same catalyst to isomerise hexitols, that is D-glucitol (sorbitol), D-mannitol and L-iditol, which are the biogenic precursors of IS, IM and II, respectively.¹⁰ Starting from a solution of D-glucitol under H₂ (>100 bar) and a base, a final 41 : 32 : 27 equilibrium mixture of D-glucitol, D-mannitol and L-iditol was achieved. More recently, van Es and co-workers reported the synthesis of II by IS isomerisation over Ru/C, leading to the same equilibrium distribution of the three isomers.⁸ Again, high H₂ pressure (40 bar) and temperature (220 °C) were necessary to reach equilibrium, and increasing the initial pH from 7 to 10 was key to improve the yield: the mass loss decreased from 25% to 6.4%. The observed by-products such as linear diols or volatile alcohols were ascribed to hydrodeoxygenation of IS, which

could be based on acid-catalysed dehydration. Pd/C, Pt/C, Rh/C and Au/C were not active, while Ru/Al₂O₃ and Ni/SiO₂ showed slightly lower activity compared to Ru/C. Isohexide isomerisation was also investigated using a homogeneous catalyst (ruthenium complexes with pincer-type phosphine ligands) in *t*-amyl alcohol.¹¹ Here also, the presence of a base (^tBuOK) enhanced the homogeneous reaction until thermodynamic equilibrium.^{11b} Nonetheless, in stark contrast to heterogeneous catalysis conditions, the reaction could be conducted without exogenous H₂.

Herein, we present a combined experimental and computational study to rationalize the role of H₂ on the isomerisation of IS over Ru/C. Particularly, we demonstrate the possibility of conducting the reaction at low H₂ pressure either in the presence of an inert gas, or using 2-propanol as hydrogen donor.

Results and Discussion

Catalytic performance

The kinetic profiles for the isomerisation of IS, IM and II at 200 °C are shown in Fig S1. Regardless of the starting isohexide, the same equilibrium distribution was reached with 59% II, 35% IS and 6% IM. *Endo*-OH groups and *exo*-OH groups could be interconverted, showing no obvious difference of reactivity. By adjusting the starting pH from 7 to 10 with 0.5 M NaOH solution at 200 °C for 1 h, the carbon balance was considerably improved, because undesired by-products were avoided (Fig S2). Increasing the reaction temperature accelerated the isomerisation towards equilibrium, but at the expense of the carbon balance (Fig S3). Notably, an external H₂ pressure was required to enable the transformation, resulting in a higher IS conversion until equilibrium (Fig 1). However, isomerisation did not require a H₂ pressure as high as reported earlier on Ni-Kieselguhr and Ru/C at comparable pH and temperature, but different types of reactors.^{7,9} This observation suggests that either the catalyst surface or reactor design can condition the reaction kinetics.

Ketones were found in trace amount in the reaction mixture (Table S1), in agreement with a dehydrogenation-rehydrogenation mechanism being regarded as responsible for isomerisation. To investigate in more detail the hydrogenation of the ketones that can participate as intermediates, two different isohexide ketone derivatives, i.e. *exo*-OH mono-ketone and isohexide di-ketone, were synthesized by oxidation of IS over a Pt-Bi/C catalyst (see ESI for details). The hydrogenation of the *exo*-OH mono-ketone preferentially formed IS as main product over Ru/C at 100 °C and 10 bar H₂ for 1 h (Fig S4a). In other words, the hydrogenation of the mono-ketone yields mainly *endo*-OH. However, partial isomerisation occurred during hydrogenation, so the other two isomers were also formed. The di-ketone could be fast converted at room temperature into a small amount of IM and a wide range of unidentified products, pointing out a high reactivity (Fig S4b).

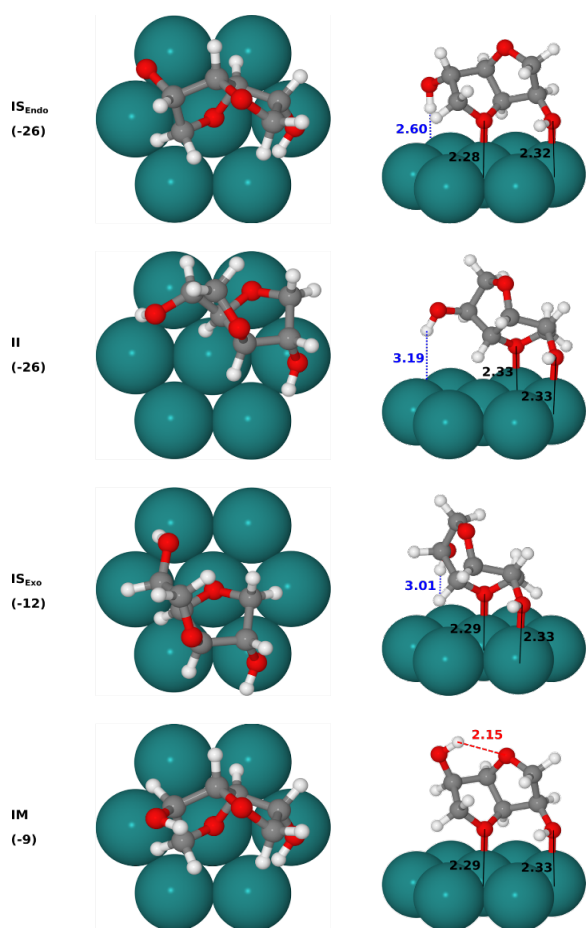


Fig 2. Adsorption modes of isohexides on Ru(0001) surface. Blue dashed lines indicate favourable agostic interaction with the surface; red dashed line represents H-bonding. Main distances are provided in Å; the numbers in parentheses are the free energy of adsorption of the corresponding isomers in $\text{kJ}\cdot\text{mol}^{-1}$ at 160 °C and 1 bar pressure.

Mechanistic investigation by periodic DFT

To understand why a high H_2 pressure is required for IS isomerisation, a computational mechanistic study was carried out. Relying on the experimental observation of ketone traces after the reaction, IS isomerisation is assumed to proceed *via* a sequential dehydrogenation-rehydrogenation mechanism, *i.e.* at any given time only one of both OH groups is dehydrogenated leading to the corresponding mono-ketone (MK) which is immediately rehydrogenated to give the (non-)isomerised product. This assumption precludes formation of the isosorbide di-ketone on the surface. We further restricted our analysis to a reaction path starting from O–H scission, followed by C–H scission, to form the chemisorbed MK (so called *alkoxy pathway*). The alternative route starting from C–H bond breaking followed by O–H scission (*alkyl pathway*) was dismissed based on previous studies of ketone hydrogenation,¹² and alcohol dehydrogenation,¹³ including IS.¹⁴ Assuming an *alkoxy pathway*, the rehydrogenation of the MK species was investigated starting exclusively at the α -C of the carbonyl group, giving alkoxy intermediates which are further hydrogenated to complete the catalytic cycle. However, the MK species have to be re-hydrogenated first on

its other face to invert the configuration at the α -C leading to the isomerised product. The calculations of the isomerisation pathways were performed both with and without the presence of co-adsorbed H atoms. The Ru catalyst was modelled by a 4-layered thick $p(4 \times 4)$ slab of Ru(0001) surface and the Gibbs free energies were computed using Density Functional Theory (DFT) at the PBE-dDsC level (see ESI for details).

Adsorption of isohexides

Adsorption of IS on the catalyst surface is the branching point towards the formation of II (hereby referred to as **Endo2Exo** pathway) or IM (**Exo2Endo** pathway). For reference, the most stable gas phase geometries of the three isomers are given in Fig S5. IS manifests different adsorption modes depending on whether adsorption takes place mainly *via* the *endo*- or *exo*-OH. In its most stable adsorption mode, IS lies parallel to the surface with the O atom of the *endo*-OH and the ether-O of the *adjoining* ring interacting with two neighbouring Ru atoms (Fig 2, **IS_{Endo}**). This adsorption mode was found to be much more stable ($G_{\text{ads}} = -26 \text{ kJ}\cdot\text{mol}^{-1}$) than a perpendicular adsorption mode where only interaction with the surface is through the *endo*-OH ($G_{\text{ads}} = +6 \text{ kJ}\cdot\text{mol}^{-1}$, Fig S5), indicating that the ether contributes a large part of the adsorption energy. Indeed, the corresponding distances show that the ether-O atom is closer (2.28 Å) to the surface than the O of the *endo*-OH group (2.32 Å). This slight tilt towards the ether also favours a weak agostic interaction between the H of the unbound *exo*-OH and the Ru surface;¹⁵ the corresponding H...Ru surface distance (2.60 Å) is indicated in blue in Fig 2. Adsorption through the *exo*-OH of IS (Fig 2, **IS_{Exo}**) involves the O atom of the *exo*-OH and the ether-O of the *same* ring lying on top of two neighbouring Ru atoms. Unlike **IS_{Endo}**, this adsorption mode is rather constrained and requires a distortion of the *exo*-OH from its most stable gas phase orientation which makes **IS_{Exo}** 14 $\text{kJ}\cdot\text{mol}^{-1}$ less stable than **IS_{Endo}**. A slight distortion from the gas phase orientation is also observed in the H atom of the unbound *endo*-OH which points away from the corresponding ring ether to better point towards the surface, thus generating a slightly favourable, albeit weaker than that in **IS_{Endo}**, agostic interaction (3.01 Å). We emphasize here that the adsorption through ether-O, be it of the *same* ring or the *adjoining* ring, is characteristic to all the reaction species involved; and a comparison of the **IS_{Endo}** and **IS_{Exo}** adsorption modes clearly demonstrates that better interaction is achieved when ether of the adjoining ring is involved in bonding with the surface.

II has both OH groups in *exo* position and thus exhibits an adsorption mode similar to **IS_{Exo}** (Fig 2, **II**). Likewise, IM has both OH groups in *endo* position and thus exhibits adsorption mode similar to **IS_{Endo}** (Fig 2, **IM**). Notably, the unbound *endo*-OH group lies farther away from the surface in a H-bonding-like interaction with the ether-O of the *adjoining* ring, precluding any agostic interaction with the surface.

Free energy profile in the limit of a low H surface concentration

To investigate the free energy profile in the limit of low H surface concentration. The chemisorbed H atoms resulting

from initial dehydrogenation were allowed to relax on separate slabs thereby making it zero co-adsorption case. The optimized geometries for all the relevant reaction intermediates (RI) and transition states (TS) are provided in Fig. 4, whereas Fig. 3 gives a plot of the free energy profiles computed for the two reaction pathways, **Endo2Exo** and **Exo2Endo**.

The two pathways follow the same sequence of steps, and differ only from the nature of the OH group that is isomerised. The first step corresponds to the initial adsorption of IS in **IS_{Endo}** (**Endo2Exo**) or **IS_{Exo}** (**Exo2Endo**) mode (Fig. 2). The initial adsorption modes then serve as reactants for the first O–H

scission TS, denoted **TS1(OH)** in Fig. 3 and Fig. 4. The overall barrier for this transformation is rather low and is roughly the same for both pathways (42–44 kJ.mol⁻¹). The **TS1(OH)** leads to very stable alkoxy intermediates, **Alkoxy1**, with the same adsorption pattern as **IS_{Endo}** and **IS_{Exo}** adsorption modes, and only differing from the location of alkoxy O which sits atop a hollow fcc site instead of a Ru atom (Fig. 4). This 3-fold hollow-site adsorption is typical of alkoxy species on Ru(0001) and renders them much more stable than their corresponding reactants. Overall, the formation of alkoxy intermediates is a highly exoenergetic transformation which should happen spontaneously.

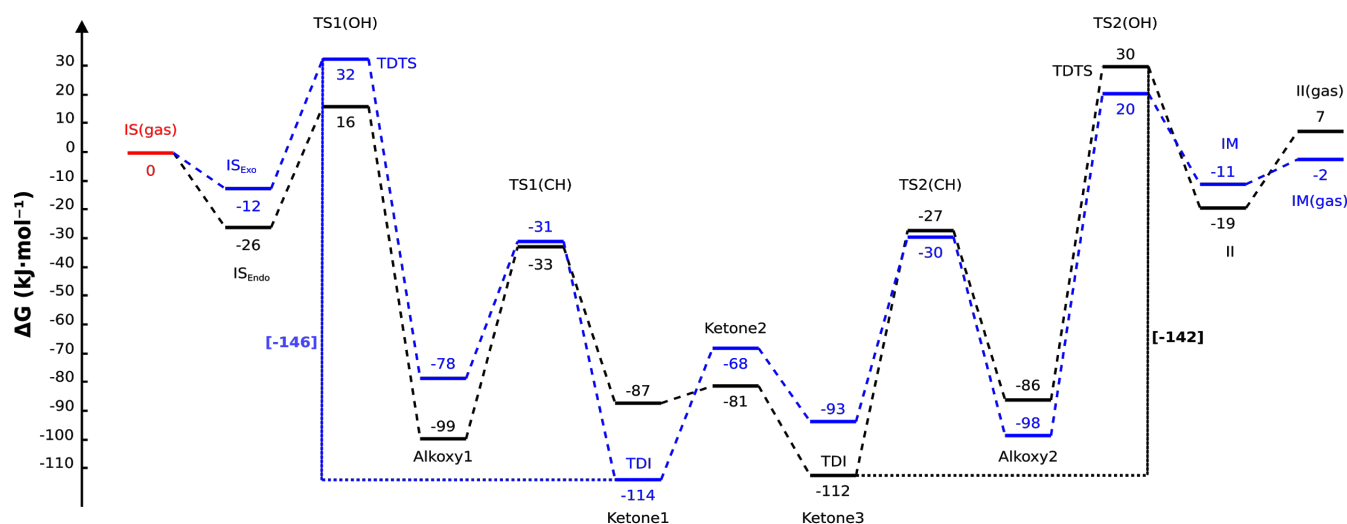


Fig. 3. Free energy profiles for IS isomerisation. The black line represents **Endo2Exo** pathway; blue line represents the **Exo2Endo** pathway. The energy spans are highlighted with dotted line. The entropic and enthalpic contributions for the adsorbates were calculated using an ideal gas harmonic approximation at 160 °C and 1 bar pressure.

Endo2Exo

Exo2Endo

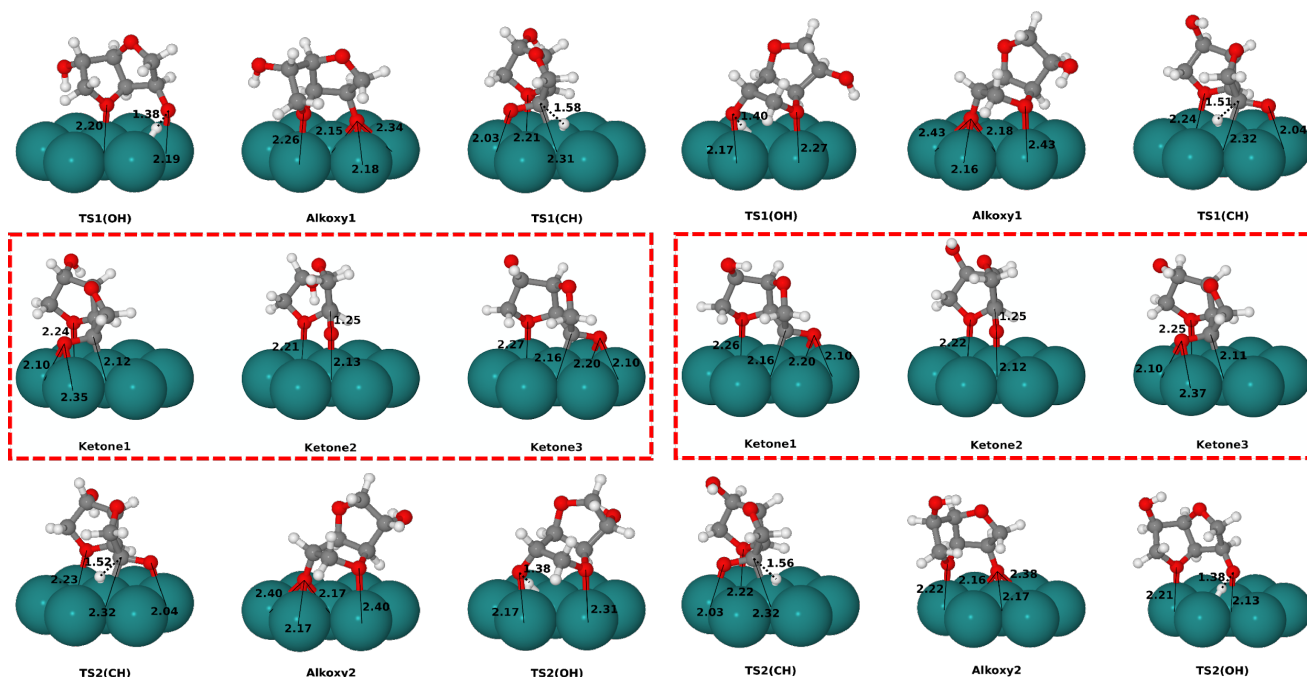


Fig. 4. Optimized structures along the **Endo2Exo/Exo2Endo** pathways. Main distances are provided in Å. Colour scheme: C in grey, H in white, O in red, Ru in green.

ARTICLE

The **Alkoxy1** intermediates further undergo C–H scission *via* **TS1(CH)** to produce MK intermediates (**Ketone1**). To reach this TS and the corresponding MK, a strong distortion is necessary to shift the alkoxy oxygen from the 3-fold hollow-site to atop a Ru atom, so that the –C=O group can lie on a bridge site in a di-sigma fashion either in front (**Endo2Exo**) or back (**Exo2Endo**) of the ring skeleton. This adsorption mode allows the α -carbon to be close enough to the surface to lose its H atom in **TS1(CH)**. This results in turn in higher barriers for CH scission compared to OH scission. We notice at this point that to isomerise the respective OH group, the rehydrogenation of MK *must* happen on the opposite side compared to the first C–H scission TS. Thus, **Ketone1** has to turn into MK RI, **Ketone2** that is chemisorbed through the ketone oxygen only and then into **Ketone3**, which is chemisorbed through the right face of the C=O bond, leading to the isomerised product by subsequent rehydrogenation. The MK intermediates are highlighted in red rectangle in Fig 4.

In the second half of the catalytic cycle, **Ketone3** RIs undergo rehydrogenation preferentially at the α -carbon to produce **Alkoxy2** intermediates, which feature an inverted symmetry at the α -carbon compared to **Alkoxy1**. This transformation involves the C–H bond-making TS, labelled as **TS2(CH)** in Fig 3 and Fig 4. Subsequent hydrogenation of **Alkoxy2** generates either II or IM. This requires crossing a very high energy barrier through the O–H bond-making TS, *i.e.* **TS2(OH)**, and is highly endoenergetic for both pathways. The eventual desorption of IM and II completes the catalytic cycle and leads to the isomerised products.

Overall, both pathways feature similar free energy profiles with the highest lying TS corresponding to the *exo*-O–H scission/formation, *i.e.* **TS1(OH)** in **Exo2Endo** and **TS2(OH)** in **Endo2Exo**, and the most stable RI being the chemisorbed (*exo*-)MK (**Ketone1** in **Exo2Endo**, **Ketone3** in **Endo2Exo**). Assuming that isomerisation of IS into II or IM is an athermic process, the energy span can be calculated as the difference of the free energy of TOF determining transition state (TDTS) and TOF determining intermediate (TDI),¹⁶ both of which are indicated on the profiles in Fig 3. The similar energy span for **Exo2Endo** and **Exo2Endo** pathways, 142 and 146 kJ.mol⁻¹, respectively, agree well with the experimental observation that there is no prominent difference in the reactivity of *endo* (*exo*)-OH groups in IS (Fig S1).

Role of ring ethers

The adsorption of MKs is discussed here in detail owing to their pivotal role in the isomerisation process. All MK RI adsorb on the surface through their carbonyl group in a top or di-sigma fashion and the ether-O of the adjoining ring. We

suspect that this adjoining-ring ether O, which is uniquely present due to the bicyclic nature of IS and its isomers, is suitably positioned relative to the carbonyl group to stabilize the MK chemisorption. To confirm this hypothesis, we looked at the dehydrogenation-rehydrogenation profile of a simpler molecule, 3-hydroxytetrahydrofuran (**3-OH-THF**), which is just one 5-membered ring of IS. Although **3-OH-THF** has a ring ether, its position relative to the OH group does not stabilize the ketone intermediates since it points away from the surface (Fig 5). In contrast, the mono-ketone intermediates of IS are more strongly adsorbed compared to those of **3-OH-THF** by >30 kJ.mol⁻¹ (Fig S6). Owing to this strong adsorption, mono-ketones probably act as a bottleneck along the isomerisation pathway in absence of H₂. This was further confirmed experimentally by a catalytic test performed in the absence of H₂ using IS and **3-OH-THF** as substrates (Table S2). While IS was found to be unreactive (no isomerisation, no production of ketones), **3-OH-THF** was reactive and a significant amount of ketone was detected after 2 h. In light of these results, we understand that IS is a unique substrate whose bicyclic nature combined with the presence of ethers in each ring contributes to the too-strong adsorption of the corresponding ketone that hinders catalytic transformation in the absence of H₂.

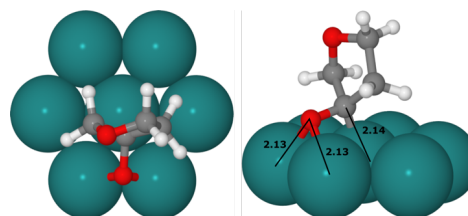


Fig 5. Most stable adsorption structures of ketone resulting from **3-OH-THF**. Left: top view; Right: side view.

Free energy profile in presence of a high H₂ pressure

The pristine catalyst surface considered above can be regarded as a low-H₂ ideal scenario. Under an external H₂ pressure, the catalyst surface can be covered by H species to varying extent. In presence of water, a competition with OH, O and H₂O is expected. Fig S7 shows the most stable distribution of H atoms on Ru(0001) at each level of coverage from 1 H atom up to a monolayer and the average free energy of adsorption at each coverage ($G_{\text{ads}}/\text{H} = -29$ kJ.mol⁻¹ for a monolayer). Fig S8 shows the predominance diagram of H/O/OH/H₂O on Ru(0001) as computed using *ab initio* thermodynamics. For a H₂ pressure above 1 bar, the Ru(0001) surface is predicted to be covered by a monolayer of H, the H₂ pressure protecting the Ru surface from partial surface oxidation.

As a natural step, the free energy profiles in Fig 3 were recomputed in the presence of explicitly co-adsorbed H. Two

coverage levels of H were considered, $\theta_H = 0.5$ ML (8 H atoms on 4x4 slab) and $\theta_H = 0.75$ ML (12 H atoms on 4x4 slab). We discarded the possibility of a fully coverage ($\theta_H = 1$ ML), since in that case, the catalyst surface cannot catalyse the C-H scission that is necessary to isomerize IS. The catalyst surface model was the same pristine surface considered in the last section, but covered with most stable distribution of H at each level of coverage. Starting from the adsorption geometries on the pristine surface (Fig 4, $\theta_H = 0$ ML), all the RS were reoptimized at the same level of theory in the presence of 8 or 12 H atoms, and a systematic approach was employed to find the most suitable adsorption sites for the co-adsorbed H atoms around RS (see ESI for details).

In general, at each θ_H coverage, H atoms prefer adsorption sites that maximize their distance from the co-adsorbed RS. At $\theta_H = 0.5$ ML, enough sites are available for H atoms to adsorb far enough from the RS to cause little to no effect on the adsorption geometry of RS. At $\theta_H = 0.75$ ML, however, H atoms have to adsorb closer to RS due to lack of space, thus inducing slight changes in the adsorption geometry. For instance, the **Alkoxy2** intermediate of the **Endo2Exo** pathway moves from a 3-fold fcc site to a 2-fold bridge site. Another effect observed at each H-coverage is the elongation of the Ru-O_{ether} distance for all species, signifying that RS, when co-adsorbed with H, lacks the stabilizing effect of ring ethers observed on the pristine surface. Coordinates for all the optimized structures both with and without co-adsorbed H are provided in the ESI.

The resulting free energy profile for **Endo2Exo** and **Exo2Endo** pathways are provided in Fig 6 and Fig S9, respectively. Since the trend as a function of the H-coverage is the same in both cases, we focus on the **Endo2Exo** pathway. Overall, the co-adsorption of H results in an upward shift of the free energy profile. However, the effect is not proportional for the different intermediates and transition states. The most drastic destabilizing effect is observed for the ketone inter-

mediates: compared to the situation at 0 ML H coverage, **Ketone3** is destabilized by 38 kJ.mol⁻¹ at 0.5 ML and by 75 kJ.mol⁻¹ at 0.75 ML. At 0.75 ML, ketones are no longer the most stable intermediates and are replaced by **Alkoxy1**. In contrast, the highest lying **TS2(OH)** is destabilized by 24 kJ.mol⁻¹ and 45 kJ.mol⁻¹ at 0.5 ML and 0.75 ML, respectively. To better understand the source of this high increase in the free energy of key RS, we performed a deformation-interaction analysis described in Scheme S1. Based on this analysis, **TS2(OH)** destabilization is the result of a sum of different small subtle effects. The high increase in the free energy of TDTs (**TS2(OH)**) and TDI (**Ketone 3**) leads to an overall decrease in the reaction span by 14 and 19 kJ.mol⁻¹ at 0.5 ML and 0.75 ML, respectively (Fig S10). This corresponds to an increase in TOF by a factor of at least 50. These findings clearly confirm the pivotal role of an external pressure of H₂ in facilitating the isomerisation of IS as observed experimentally (Fig 1). The driving phenomenon is to limit catalyst poisoning by strongly chemisorbed MKs. At high coverage, MKs even become less stable than **Alkoxy1**. Remarkably, the limiting transition is **TS2(OH)** that corresponds to the re-hydrogenation process.

Effect of an inert gas

The experiments and calculations above point out a relevant role of H₂ in the IS isomerisation kinetics over Ru/C. To further ascertain how the H₂ partial pressure influences the reaction, an inert gas (*i.e.* N₂ or He) was added to the reactor at different pressures (Table 1). Surprisingly, a clear promoting effect is observed. When the starting H₂ pressure is 6 bar, the IS conversion is only 16% after 2 h (entry 1). However, when additional N₂ or He (30 bar) is charged into the reactor, equilibrium is attained under otherwise identical conditions (entries 2 and 3). A similar effect is observed when a lower H₂ pressure (2 bar) is applied (entries 4-6). For comparison, control experiments with either pure N₂ or He (about 30 bar) did not show appreciable activity (entries 7 and 8).

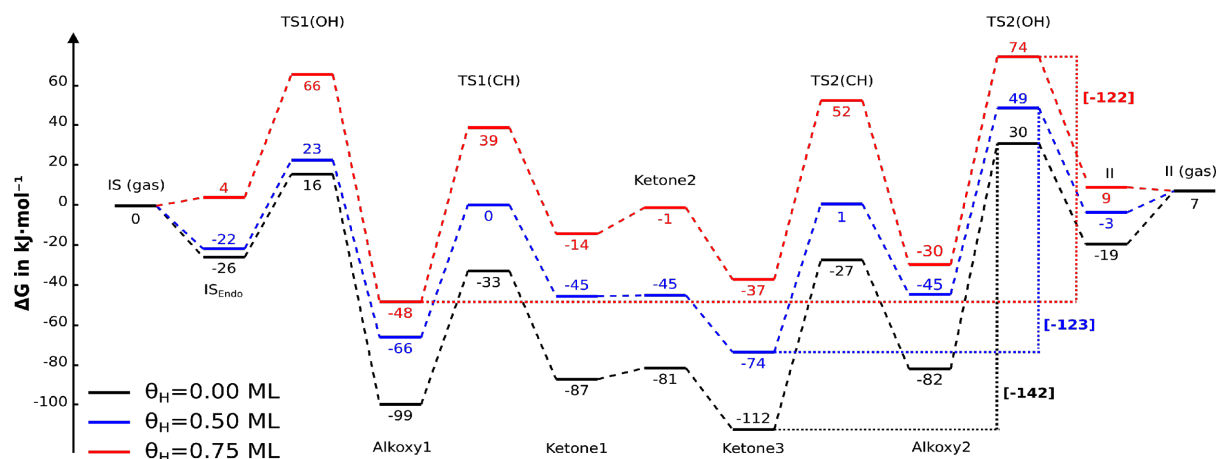


Fig 6. Free energy profiles for the **Endo2Exo** pathway at different surface concentrations of co-adsorbed H. The first and last points represent IS and II in the gas phase along with the Ru(0001) at different H coverage: 0 ML in black, 0.5 ML (8 H/supercell) in blue, 0.75 ML (12 H/supercell) in red. The two H atoms resulting from initial dehydrogenation were allowed to relax each on a separate H covered surface with 0, 8 or 12 H atoms. The energy spans are indicated by dotted lines. The entropic and enthalpic contributions for the adsorbates were calculated using an ideal gas approximation at 160 °C and 1 bar pressure.

ARTICLE

Table 1. Effect of inert gases on IS isomerisation in water

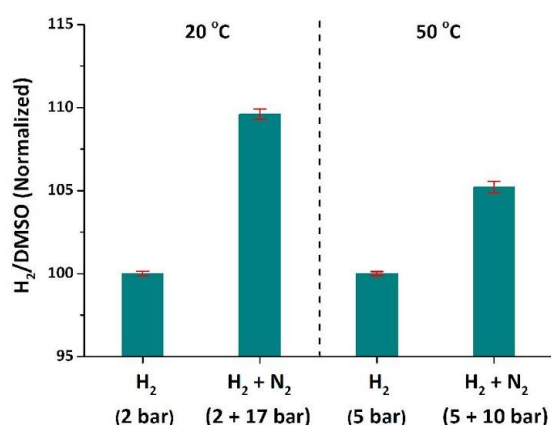
Entry	Pressure start (bar)			Pressure at target T (bar)	Pressure after reaction (bar)	Ratio IS:II:IM	CB (%)
	H ₂	N ₂	He				
1	6	-	-	17	6	84 : 12 : 4	97
2	6	30	-	65	35	37 : 56 : 7 (eq.)	92
3	6	-	30	57	36	36 : 58 : 6 (eq.)	92
4	2	-	-	15	2	98 : 2 : 0	100
5	2	31	-	62	33	50 : 43 : 7	97
6	2	-	30	54	33	48 : 46 : 5	99
7	-	31	-	57	32	100 : 0 : 0	97
8	-	-	30	50	30	100 : 0 : 0	98

Reaction conditions: 1 g IS, 15 mL H₂O, pH 10, 0.05 g Ru/C, 200 °C, 2 h

Table 2. IS isomerisation in 2-propanol (IPA)

Entry	IPA (%)	H ₂ O (%)	IPA / IS (mol:mol)	Pressure start (bar)		Pressure at target T (bar)	Pressure after reaction (bar)	Ratio IS:II:IM	CB (%)
				H ₂	N ₂				
1	100	-	28.6	3	-	33	13	86 : 12 : 2	104
2	100	-	28.6	11	-	39	18	74 : 21 : 5	101
3	100	-	28.6	31	-	39	31	37 : 57 : 6	103
4 ^[a]	100	-	-	-	2	33	14	-	-
5	100	-	28.6	-	2	33	15	89 : 9 : 2	99
6	50	50	14.3	-	2	31	12	78 : 17 : 5	105
7	40	60	11.5	-	2	32	10	73 : 22 : 5	106
8	30	70	8.6	-	2	29	9	76 : 19 : 5	99
9	20	80	5.7	-	2	25	7	76 : 19 : 5	102
10	10	90	2.9	-	2	18	8	99 : 1 : 0	102
11	-	100	-	-	2	8	2	100 : 0 : 0	101
12	40	60	11.5	-	11	39	17	57 : 36 : 7	97
13	40	60	11.5	-	31	72	35	49 : 43 : 8	94
14	40	60	11.5	-	51	103	55	47 : 45 : 8	91
15 ^[b]	40	60	11.5	-	31	73	35	37 : 57 : 6	92

Reaction conditions: 1 g IS, 15 mL solvent, 0.05 g Ru/C, 200 °C, 2 h; ^[a] in absence of substrate, ^[b] 4 h.

**Fig 7.** Effect of N₂ on the relative H₂ solubility measured by ¹H NMR using DMSO as internal standard.

The promoting role of N₂ on IS isomerisation can be rationalised at first sight by the formation of N₂H and N₂H₂ species on metal Ru. Such a mechanism has been proposed to

explain the 4.3-fold increase of activity in the hydrodeoxygenation of *p*-cresol to toluene over Ru/TiO₂ by introducing 6 bar N₂ in batch conditions at 160 °C and 1 bar H₂.¹⁷ While this mechanism could occur during IS isomerisation in the presence of N₂, the promoting effect also observed under He, which is a fully inert gas, discourages this option. It is known that the gas-liquid interfacial tension decreases with the total gas pressure, resulting in larger interfacial areas, and in turn into an enhanced H₂ transfer from the gas to the liquid phase.¹⁸ Also, the presence of a second gas can enhance the H₂ solubility as suggested by Maxwell-Stefan equations for multicomponent diffusion (see ESI). To assess how the H₂ solubility is affected by an inert gas, a series of H₂ solubility tests was carried out in a pressurized NMR tube in D₂O with/without N₂, using DMSO (100 ppm) as internal standard (see ESI). The relative H₂ solubility was measured at 20 °C / 2 bar H₂ and 50 °C / 5 bar H₂ and the standard deviation for a sample set of data is given in Fig 7. The excess H₂ solubility was 9.6% and 5.2% in the presence of 17 bar and 10 bar N₂, respectively. Additional results can be found in Fig S11-S14 (ESI), whereas

characteristic ^1H NMR spectra of IM, IS and II in the presence of D_2O are plotted in Fig S15-S17 (ESI). Although the enhancement of H_2 solubility promoted by N_2 is moderate, this higher H_2 solubility is expected to facilitate the equilibrium between the H-surface species and H_2 in the gas phase, yielding possibly an effective increase of the H-coverage on Ru, and accelerating in turn the isomerisation kinetics according to the mechanistic investigation above.

Isopropanol as solvent and H-donor

The effect of the solvent on IS isomerisation was also investigated (Fig 8). First, pure IS can be isomerised without any solvent with excellent carbon balance. Second, to afford a good IS solubility, several solvents with high polarity were tested. Primary alcohols or ethanol-water mixture inhibit the reaction, most likely due to competitive adsorption between the solvent and IS,¹⁹ which results in Ru/C deactivation. In contrast, isopropanol (IPA) and t-amyl alcohol promote the reactivity and the carbon balance. Notably, in the presence of IPA, a pressure increase in the autoclave was observed after reaction due to H_2 generation ascribed to IPA dehydrogenation. This observation points out that, despite H_2 generation, is it possible that IPA could contribute to isomerisation as a hydrogen transfer agent.

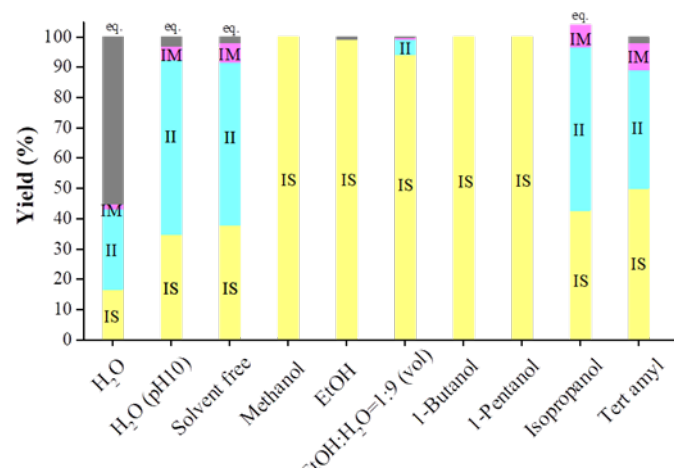


Fig 8. Product distribution and mass loss in different solvents. Reaction conditions (with solvent): 1 g IS, 15 mL solvent, 0.05 g Ru/C (5wt %), 30 bar H_2 , 200 °C, 2 h. Reaction conditions (solvent free): 15 g IS, 0.4 g Ru/C (5wt %), 30 bar H_2 , 200 °C, 2 h.

The isomerisation of IS in IPA was further performed at variable H_2 pressures (Table 2, entries 1-3). Clearly, an external H_2 pressure still exerts a positive effect on the IS conversion. However, the kinetics of isomerisation in IPA is slightly slower than in water, probably due to competitive adsorption between IPA and IS. Hence, the use of IPA/ H_2O mixtures as solvent might be a promising strategy to combine the advantages of IPA as H source and H_2O as solvent for isomerisation. We conducted IS isomerisation with IPA/ H_2O solutions under 2 bar N_2 without H_2 (entries 5-11). By decreasing the IPA ratio to less than 50%, higher IS conversion is observed with a minimum ratio of 20% to activate the reaction. Keeping the IPA ratio at 40%, the N_2 pressure was increased (entries 12-

14). The IS conversion increases proportionally with the N_2 pressure, but the promoting effect is not significant when the pressure exceeds 30 bar. Final equilibrium with good carbon balance was obtained under 31 bar N_2 after 4 h (entry 15). One can mention a slight increase of the total pressure during the reaction which is ascribed to the generation of H_2 from IPA dehydrogenation (entries 12-14). To confirm this hypothesis, the IS isomerisation reaction was carried out at variable temperature and time combinations using 40 % IPA and 60 % H_2O (Table S3). The final reaction mixtures were analysed by ATR-IR, and acetone was detected as dehydrogenation product (Fig S18). In summary, IS isomerisation can occur with IPA as a H-donor and N_2 as a promoter without adding external H_2 .

Conclusions

The kinetics of isosorbide isomerisation is very sensitive to the H_2 pressure. This effect can be primarily ascribed to lateral interactions between the transition states, the intermediate ketones and the adsorbed H species over metal Ru, especially at full H-coverage, as inferred from DFT calculations. In the absence of co-adsorbed H, chemisorbed mono-ketones are strongly bonded to the Ru surface because of the stabilizing interaction with the ether of the adjoining cycle. As a result, mono-ketones poison the Ru catalyst in the absence of H_2 , the re-hydrogenation being the limiting process. In presence of H_2 , mono-ketones are less strongly adsorbed and are more easily re-hydrogenated, producing IS, IM or II depending on the adsorption mode. Another possible effect of the H_2 pressure is to protect the Ru surface, limiting partial oxidation by water. The addition of an inert gas (i.e. N_2 or He) or the use of isopropanol as co-solvent can promote the reactivity by enhancing the kinetics of H_2 solubilisation, and hence the H-transfer on metal Ru, respectively, with excellent carbon balance. The results presented in this study open up promising perspectives for engineering cheaper and safer processes for reactions encompassing isohexides.

Author Contributions

HH: Data curation, formal analysis, investigation, methodology, visualization, writing original draft; AR: Data curation, formal analysis, investigation, methodology, software, visualization, writing original draft; RW: formal analysis, methodology, software, validation, writing – review & editing; FJ: formal analysis, methodology, validation, writing – review & editing; CM: conceptualization, funding acquisition, resources, supervision, validation, writing original draft, writing – review & editing; KOV: conceptualization, resources, supervision, validation, writing original draft, writing – review & editing; MPT: conceptualization, funding acquisition, project administration, resources, supervision, validation, visualization, writing original draft, writing – review & editing

Conflicts of interest

“There are no conflicts to declare”.

Acknowledgements

The authors express their gratitude to Solvay for funding. This work has been realized with the financial support of the IDEXLYON project of the Université de Lyon in the framework of the Projet d'Investissement d'Avenir (ANR-16-IDEX-0005), as well as SYSPROD and Axelera Pole de Competitivite (PSMN Data Center). This study also received granted access to the HPC resources of CINES and IDRIS under the allocation 0800609 made by GENCI. The authors would like to thank Dimitri Wietthoff for the support on the operation of catalytic apparatus.

References

- (a) G. Flèche and M. Huchette, *Starch/Stärke*, 1986, **38**, 26; (b) M. Rose and R. Palkovits, *ChemSusChem*, 2012, **5**, 167; (c) I. Delidovich, P. Hausoul, L. Deng, R. Pfützenreuter, M. Rose and R. Palkovits, *Chem. Rev.*, 2016, **116**, 1540.
- (a) F. Fenouillot, A. Rousseau, G. Colomines, R. Saint-Loup and J. P. Pascault, *Progr. Polym. Sci.*, 2010, **35**, 578; (b) V. Froidevaux, C. Negrell, S. Caillol, J. P. Pascault and B. Boutevin, *Chem. Rev.*, 2016, **116**, 14181.
- (a) L. F. Wiggins, *J. Chem. Soc.*, 1945, 4; (b) R. Montgomery and L. F. Wiggins, *J. Chem. Soc.*, 1946, 390; (c) H. G. Fletcher and R. M. Goepf, *J. Am. Chem. Soc.*, 1946, **68**, 939; (d) H. G. Fletcher Jr, and R. M. Goepf Jr, *J. Am. Chem. Soc.*, 1945, **67**, 1042.
- A. C. Cope and T. Y. Shen, *J. Am. Chem. Soc.*, 1956, **78**, 31773182.
- S. Brimacombe, A. B. Foster, M. Stacey and D. H. Whiffen, *Tetrahedron* 1958, **4**, 351.
- (a) L. W. Wright and J. D. Brandner, *J. Org. Chem.*, 1964, **29**, 2979-2982; (b) D. Brandner and L. W. Wright, US3023223A, 1962.
- (a) R. U. Lemieux and A. G. McInnes, *Can. J. Chem.*, 1960, **38**, 136; (b) P. Tundo, F. Aricò, G. Gauthier, L. Rossi, A. Rosamilia, H. S. Bevinakatti, R. L. Sievert and C. P. Newman, *ChemSusChem*, 2010, **3**, 566; (d) R. Pruvost, J. Boulanger, B. Léger, A. Ponchel, E. Monflier, M. Ibert, A. Mortreux, T. Chenal and M. Sauthier, *ChemSusChem*, 2014, **7**, 3157; (d) R. Pfützenreuter and M. Rose, *ChemCatChem*, 2016, **8**, 251.
- J. L. Nôtre, J. van Haveren and D. S. van Es, *ChemSusChem*, 2013, **6**, 693.
- R. V. Engel, J. Niemeier, A. Fink and M. Rose, *Adv. Synth. Catal.*, 2018, **360**, 2358.
- L. Wright and L. Hartmann, *J. Org. Chem.*, 1961, **26**, 1588-1596
- D. Pinggen, O. Diebolt and D. Vogt, *ChemCatChem*, 2013, **5**, 2905-2912; (b) I. Vanbesien, T. Delaunay, V. Wiatz, S. Bigot, H. Bricout, S. Tilloy and E. Monflier, *Inorg. Chim. Acta*, 2021, **515**, 120094.
- C. Michel, J. Zaffran, A. M. Ruppert, J. Matras-Michalska, M. Jedrzejczyk, J. Grams and P. Sautet, *Chem. Commun.*, 2014, **50**, 12450.
- J. Zaffran, C. Michel, F. Delbecq and P. Sautet, *J. Phys. Chem. C*, 2015, **119**, 12988.
- A. Dumon, Thesis, Selective Alcohol Amination: Theoretical Study for the Design of Innovative Heterogeneous Catalysts, École Normale Supérieure de Lyon, 2016.
- (a) M. Brookhart, M. L. H. Green and G. Parkin, *Proc. Nat. Acad. Sci. USA*, 2007, **104**, 6908-6914; (b) C. Michel, F. Göttl and P. Sautet, *Phys. Chem. Chem. Phys.*, 2012, **14**, 15286.
- S. Kozuch and S. Shaik, *Acc. Chem. Res.* 2011, **44**, 101.
- H. Duan, J.-C. Liu, M. Xu, Y. Zhao, X.-L. Ma, J. Dong, X. Zheng, J. Zheng, C. S. Allen, M. Danaie, Y.-K. Peng, T. Issariyakul, D. Chen, A. I. Kirkland, J.-C. Buffet, J. Li, S. C. E. Tsang and D. O'Hare, *Nat. Catal.*, 2019, **2**, 1078.
- (a) H. H. Uhlig, *J. Phys. Chem.*, 1937, **41**, 1215; (b) R. Massoudi and A. D. King Jr, *J. Phys. Chem.*, 1974, **78**, 2262.
- M. Kennema, I. B. D. de Castro, F. Meemken and R. Rinaldi, *ACS Catal.*, 2017, **7**, 2437.